

Photocatalytic Hydrogen Evolution Using 9-Phenyl-10-methyl-acridinium Ion Derivatives as Efficient Electron Mediators and Ru-Based Catalysts

Yusuke Yamada,^A Kentaro Yano,^A and Shunichi Fukuzumi^{A,B,C}

^ADepartment of Material and Life Science, Graduate School of Engineering, Osaka University, ALCA, Japan Science and Technology Agency (JST), Suita, Osaka 565-0871, Japan.

^BDepartment of Bioinspired Science, Ewha Womans University, Seoul 120-750, Korea.

^CCorresponding author. Email: fukuzumi@chem.eng.osaka-u.ac.jp

Photocatalytic hydrogen evolution has been performed by photoirradiation ($\lambda > 420$ nm) of a mixed solution of a phthalate buffer and acetonitrile (MeCN) (1:1 (v/v)) containing EDTA disodium salt (EDTA), $[\text{Ru}^{\text{II}}(\text{bpy})_3]^{2+}$ (bpy = 2,2'-bipyridine), 9-phenyl-10-methylacridinium ion (Ph-Acr⁺-Me), and Pt nanoparticles (PtNPs) as a sacrificial electron donor, a photosensitizer, an electron mediator, and a hydrogen-evolution catalyst, respectively. The hydrogen-evolution rate of the reaction system employing Ph-Acr⁺-Me as an electron mediator was more than 10 times higher than that employing a conventional electron mediator of methyl viologen. In this reaction system, ruthenium nanoparticles (RuNPs) also act as a hydrogen-evolution catalyst as well as the PtNPs. The immobilization of the efficient electron mediator on the surface of a hydrogen-evolution catalyst is expected to enhance the hydrogen-evolution rate. The methyl group of Ph-Acr⁺-Me was chemically modified with a carboxy group (Ph-Acr⁺-CH₂COOH) to interact with metal oxide surfaces. In the photocatalytic hydrogen-evolution system using Ph-Acr⁺-CH₂COOH and Pt-loaded ruthenium oxide nanoparticles (Pt/RuO₂NPs) as electron donor and hydrogen-evolution catalyst, respectively, the hydrogen-evolution rate was 1.5–2 times faster than the reaction system using Ph-Acr⁺-Me as an electron mediator. On the other hand, no enhancement in the hydrogen-evolution rate was observed in the reaction system using Ph-Acr⁺-CH₂COOH with PtNPs. Thus, the enhancement of hydrogen-evolution rate originated from the favourable interaction between Ph-Acr⁺-CH₂COOH and RuO₂NPs. These results suggest that the use of Ph-Acr⁺-Me as an electron mediator enables the photocatalytic hydrogen evolution using PtNPs and RuNPs as hydrogen-evolution catalysts, and the chemical modification of Ph-Acr⁺-Me with a carboxy group paves the way to utilise a supporting catalyst, Pt loaded on a metal oxide, as a hydrogen-evolution catalyst.

Manuscript received: 19 June 2012.

Manuscript accepted: 1 August 2012.

Published online: 13 September 2012.

Introduction

Hydrogen has been a promising candidate as a clean fuel of the next generation to reduce consumption of fossil fuels, because completely harmless water is the only product after hydrogen burns.^[1–4] However, most hydrogen supplied for industry is currently produced from natural gas, which is composed of light alkanes, by a steam reforming reaction at high temperature, followed by high-temperature and low-temperature water–gas-shift reactions with emission of carbon dioxide that is regarded as a typical greenhouse gas.^[5] Photocatalytic hydrogen production seems to be the most environmentally benign method to produce hydrogen without emission of green house gases.^[4,6–8]

Photocatalytic hydrogen production by using a sacrificial electron donor has been extensively studied since the late 1970s.^[9–18] A typical reaction system is composed of several components; EDTA disodium salt (EDTA), $[\text{Ru}^{\text{II}}(\text{bpy})_3]^{2+}$ (bpy = 2,2'-bipyridine), methyl viologen (MV²⁺), and colloidal platinum particles (PtNPs) as a sacrificial electron donor, a photosensitizer, an electron mediator, and a hydrogen-evolution catalyst, respectively.^[9g,19] In this reaction system, the choice of

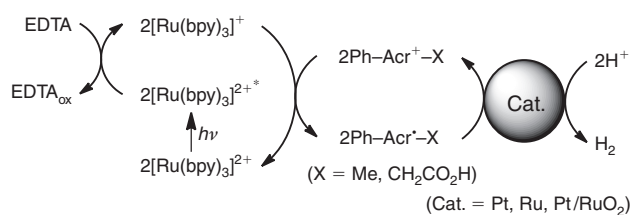
an electron mediator is generally crucial to achieve high efficiency for the photocatalytic hydrogen evolution. The electron mediator oxidatively quenches the photoexcited sensitizer, thereby creating the charge separation. Although MV²⁺ and a variety of quaternary bipyridines (viologens) have been examined as electron mediators,^[20,21] the instability of these compounds during photocatalytic hydrogen evolution has been problematic to improve.^[22] In addition, the electron-transfer rate from the photoexcited state of $[\text{Ru}(\text{bpy})_3]^{2+}$ to viologens highly depends on the reduction potentials of viologens, however, no simple correlation was found between the hydrogen-evolution rates and the redox potentials of viologens.^[20,21] Thus, various types of electron mediators such as cobalt^[23–25] and rhodium^[26–28] complexes as well as graphene oxide^[29] have been investigated as electron mediators. An ideal electron mediator should possess properties such as efficient quenching of a photoexcited sensitizer and slow back electron transfer to the sensitizer.

With regard to hydrogen-evolution catalysts PtNPs are most frequently used, because Pt has a low overpotential for proton reduction to evolve hydrogen.^[30] However, the use of Pt metals

is strongly desired to be avoided because of its high price and scarce stocks. Development of hydrogen-evolution catalysts mainly composed of inexpensive and abundant metals has merited considerable interest.^[31–34] A popular method to reduce the use of Pt metals is supporting small Pt particles on a metal oxide. Metal-oxide surfaces of a catalyst support are beneficial compared with metal surfaces to be functionalized by organic molecules possessing an acid group such as a carboxylate group. However, Pt/TiO₂ has so far been the only supporting catalyst examined in photocatalytic hydrogen evolution.^[35] This is probably because oxygen atoms interacting with Pt particles withdraw electrons from the Pt particles to decrease their electron density, resulting in deactivation of Pt particles in proton reduction.

An efficient electron mediator suitable for fast hydrogen evolution may enable utilisation of a metal oxide to support Pt particles as a hydrogen-evolution catalyst. In addition, such an electron mediator could also allow the use of non-Pt metal particles such as ruthenium, nickel, or iron particles as hydrogen-evolution catalysts.^[36–40] However, such a combination of an ideal electron mediator and a metal-oxide catalyst supporting Pt particles or non-platinum hydrogen-evolution catalysts has yet to be reported.

We report herein a photocatalytic hydrogen-evolution system using 9-phenyl-10-methyl-acridinium ion (Ph-Acr⁺-Mes)^[41]



Scheme 1. The overall catalytic cycle for the photocatalytic hydrogen evolution with EDTA, [Ru(bpy)₃]²⁺, metal or metal oxide nanoparticles (PtNPs, RuNPs or Pt/RuO₂NPs), and an electron mediator (Ph-Acr⁺-Me or Ph-Acr⁺-CH₂CO₂H).

as an efficient electron mediator together with EDTA, [Ru(bpy)₃]²⁺, and PtNPs as a sacrificial electron donor, a photosensitizer, and a hydrogen-evolution catalyst, respectively (Scheme 1). This is the first report using Ph-Acr⁺-Mes as an electron mediator in a photocatalytic hydrogen-evolution system. The 9-phenyl-10-methylacridinyl radical (Ph-Acr[•]-Mes), which is formed by the quenching of photoexcited *[Ru(bpy)₃]²⁺ by Ph-Acr⁺-Mes, has been reported to act as a strong reductant with the oxidation potential of $E^0 = -0.55$ V versus SCE in acetonitrile.^[41] This strong reducing ability of the Acr[•] moiety allows us to use not only ruthenium metal nanoparticles (RuNPs) but also ruthenium oxide nanoparticles supporting Pt particles (Pt/RuO₂NPs) as hydrogen-evolution catalysts. In order to improve the hydrogen-evolution rate of the reaction system using Ru-based catalysts, Ph-Acr⁺-Mes was chemically modified and immobilized on the surface of RuNPs and Pt/RuO₂NPs.

Results and Discussion

Photocatalytic Hydrogen Evolution Using Ph-Acr⁺-Me as an Electron Mediator

Photocatalytic hydrogen evolution was performed by photoirradiation of a mixed solution (2.0 mL) of a phthalate buffer (pH 4.5) and MeCN (1 : 1 (v/v)) containing EDTA (1.0 mM), [Ru^{II}(bpy)₃]²⁺ (0.20 mM), Ph-Acr⁺-Me (0.30 mM), and PtNPs (12.5 mg L⁻¹) as a sacrificial electron donor, a photosensitizer, an electron mediator, and a hydrogen-evolution catalyst, respectively. Fig. 1a compares the time courses of hydrogen evolution in the reaction system using Ph-Acr⁺-Me or methylviologen (MV²⁺) as an electron mediator. No hydrogen evolution was confirmed in the absence of an electron mediator or photoirradiation in advance. When MV²⁺ was used as an electron mediator, the initial hydrogen-evolution rate (60 min) was 7.1 μmol s⁻¹ g_{Pt}⁻¹, whereas the initial hydrogen-evolution rate (10 min) was as high as 92 μmol s⁻¹ g_{Pt}⁻¹ when Ph-Acr⁺-Me was employed as an electron mediator. Thus, Ph-Acr⁺-Me acts as a much more efficient electron mediator than MV²⁺. The final amount of evolved hydrogen (2.0 μmol) with Ph-Acr⁺-Me

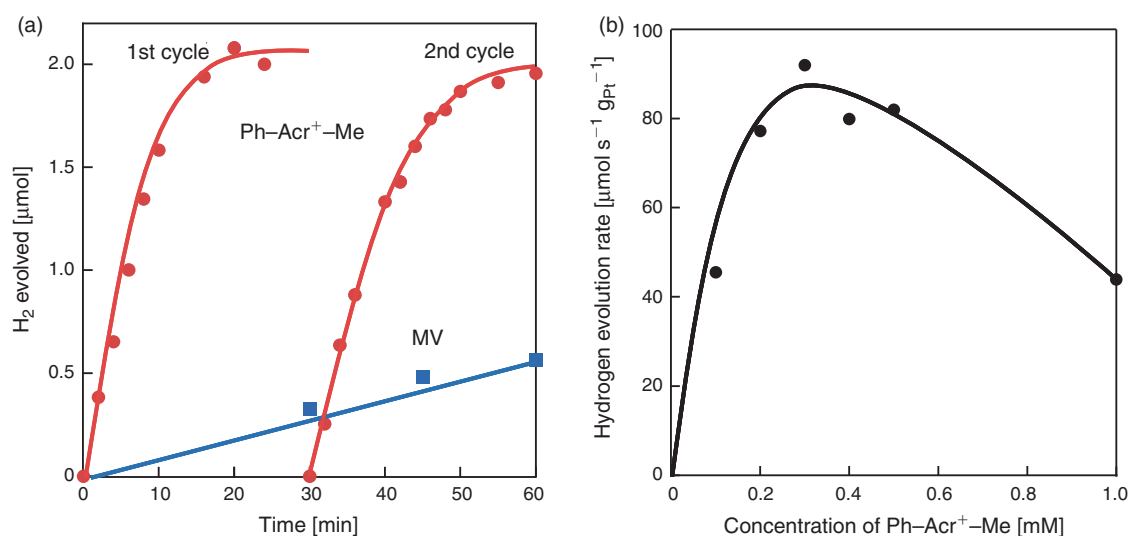


Fig. 1. (a) Time courses of hydrogen evolution by photoirradiation of a mixed solution of a phthalate buffer solution (pH 4.5) and MeCN (1 : 1 (v/v)) containing [Ru(bpy)₃]²⁺ (0.20 mM), EDTA (1.0 mM), PtNPs (12.5 mg L⁻¹), and Ph-Acr⁺-Me (0.30 mM, red circles) or methylviologen (0.30 mM, blue squares). An additional amount of EDTA (1.0 mM) was added to the solution containing Ph-Acr⁺-Me after H₂ evolution ceased. (b) Concentration effect of Ph-Acr⁺-Me on hydrogen-evolution rate.

is the same as the amount of EDTA (2.0 μmol) in the reaction solution, indicating that EDTA acts as a two-electron donor. An additional amount of EDTA (1.0 mM) was added to the solution containing Ph-Acr⁺-Me after hydrogen evolution ceased. The time course of hydrogen evolution from the solution is indicated as the second cycle in Fig. 1a. A similar hydrogen-evolution rate at the second cycle to that of the first cycle assures that Ph-Acr⁺-Me acts as a robust electron mediator. The concentration effect of Ph-Acr⁺-Me on the hydrogen-evolution rate was examined by changing the concentration within a range from 0.10 to 1.0 mM. As indicated in Fig. 1b, the hydrogen-evolution rate increases with increasing the concentration to 0.3 mM. However, the hydrogen-evolution rate decreased by increasing the concentration of Ph-Acr⁺-Me to 1.0 mM. The decrease in the hydrogen-evolution rate at the higher concentration of Ph-Acr⁺-Me is ascribed to light absorption due to Ph-Acr⁺-Me, which disturbs the photoexcitation of [Ru(bpy)₃]²⁺ (UV-vis spectra of Ph-Acr⁺-Me and [Ru(bpy)₃]²⁺ are shown in Fig. A1 in the Supplementary Material). Thus, the concentrations of [Ru(bpy)₃]²⁺ and Ph-Acr⁺ derivatives were fixed as 0.2 and 0.3 mM, respectively, for further investigation.

Preparation of Ru-Based Catalysts

Platinum nanoparticles are known as an efficient catalyst for hydrogen evolution. However, the high cost and scarce stocks limit their use in any industrial applications. As an alternative

catalyst, RuNPs^[36a] and RuO₂NPs^[38–40] have been reported to act as an efficient hydrogen-evolution catalysts in the photocatalytic hydrogen-evolution system. Thus, both RuNPs and RuO₂NPs were examined instead of PtNPs in the photocatalytic hydrogen-evolution system using Ph-Acr⁺-Me as an electron mediator.

RuNPs were prepared by the reduction of RuCl₃ with NaBH₄ in an aqueous solution (see Experimental section). The obtained RuNPs were characterised by transmission electron microscopy (TEM) as shown in Fig. 2a. The size of the primary particles of RuNPs was around 4 nm. A powder X-ray diffraction pattern of the RuNPs is displayed in Fig. 2c. The strong peak around 42° assignable to metallic Ru is clearly observed.^[42a]

RuO₂NPs were prepared by calcination of the RuNPs at 600°C for 4 h in air. The size of the RuO₂NPs was confirmed by TEM observation to be $\sim 20 \text{ nm} \times \sim 7 \text{ nm}$. Formation of RuO₂ in the rutile-type structure was confirmed by the powder X-ray diffraction pattern as indicated in Fig. 2d. The peaks at 29°, 35°, 40°, 41°, and 54° are indexed to (110), (101), (200), (111), and (211) planes, respectively.^[42b] The small sizes of the RuNPs and RuO₂NPs assure high dispersity in the reaction solution by ultrasonication.

Photocatalytic Hydrogen Evolution with Ph-Acr⁺-Me and RuNPs or RuO₂NPs

The photocatalytic hydrogen evolution was conducted using RuNPs (0.10 g L⁻¹) or RuO₂NPs (0.25 g L⁻¹) as hydrogen-

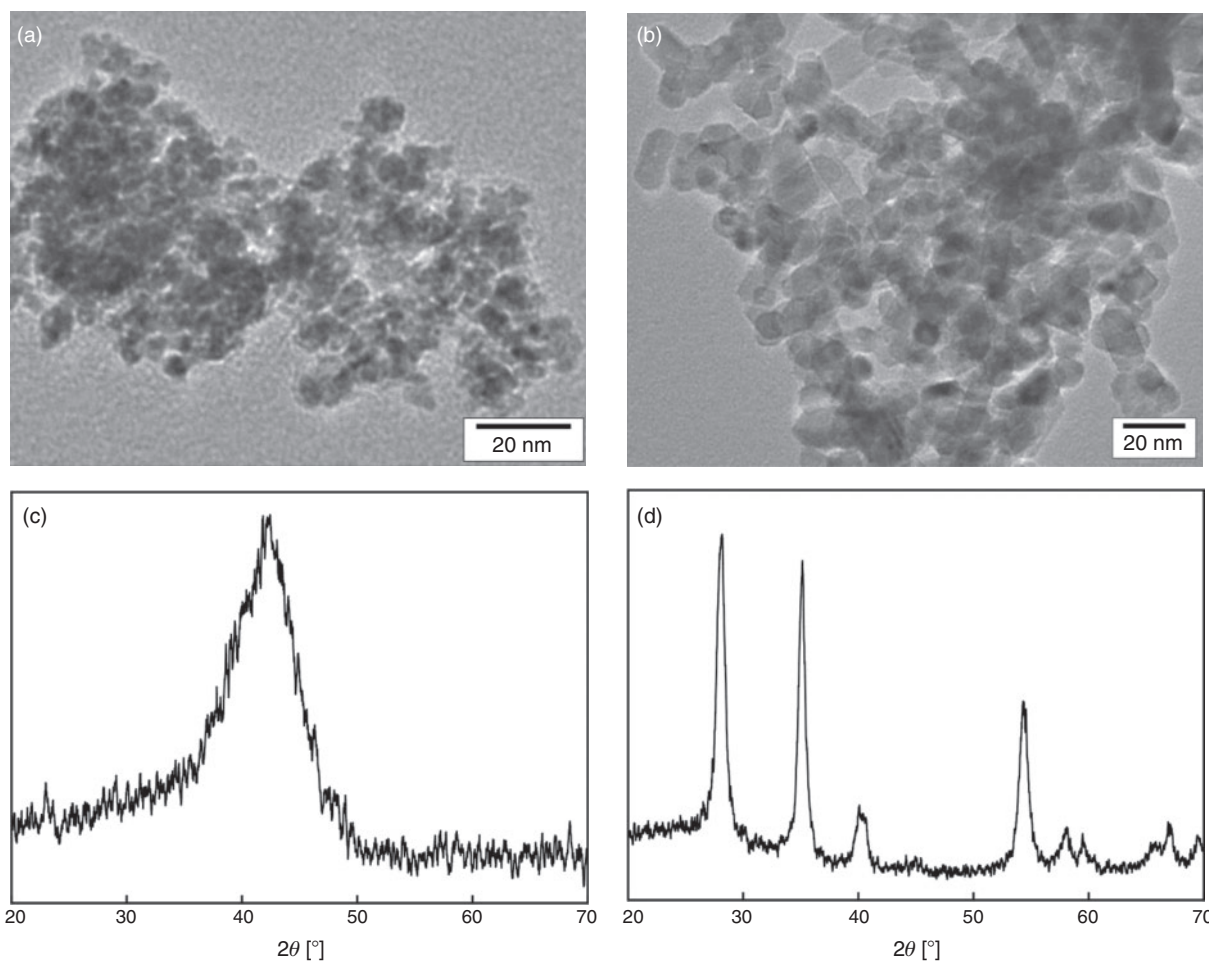


Fig. 2. Transmission electron microscopy images of (a) RuNPs and (b) RuO₂NPs. X-ray diffraction patterns of (c) RuNPs and (d) RuO₂NPs.

evolution catalysts by photoirradiation ($\lambda > 420$ nm) of a mixed solution of a phthalate buffer (pH 4.5) and MeCN (1 : 1, (v/v)) containing $[\text{Ru}(\text{bpy})_3]^{2+}$ (0.20 mM), EDTA (1.0 mM), and Acr^+-Ph (0.30 mM) as a photosensitizer, a sacrificial electron donor, and an electron mediator, respectively. Hydrogen evolution was observed in both the reaction systems using RuNPs and RuO_2NPs as hydrogen-evolution catalysts (Fig. A2 in the Supplementary Material). The hydrogen-evolution rate of the reaction system using PtNPs and $\text{Ph}-\text{Acr}^+-\text{Me}$ as hydrogen-evolution catalyst and an electron mediator is as high

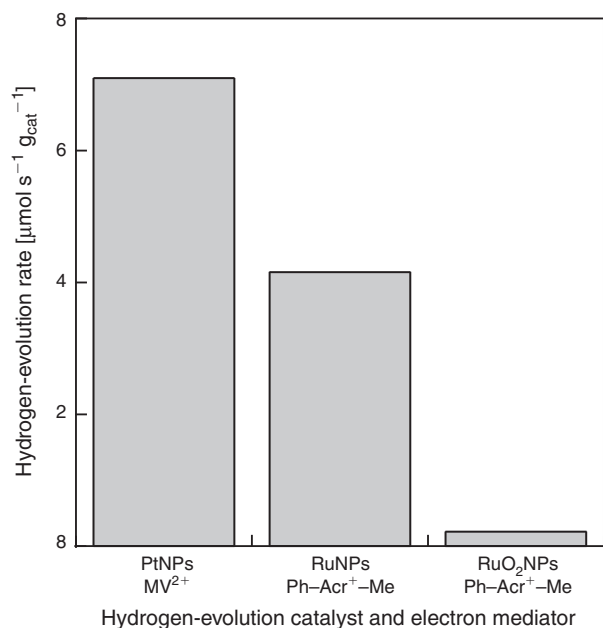
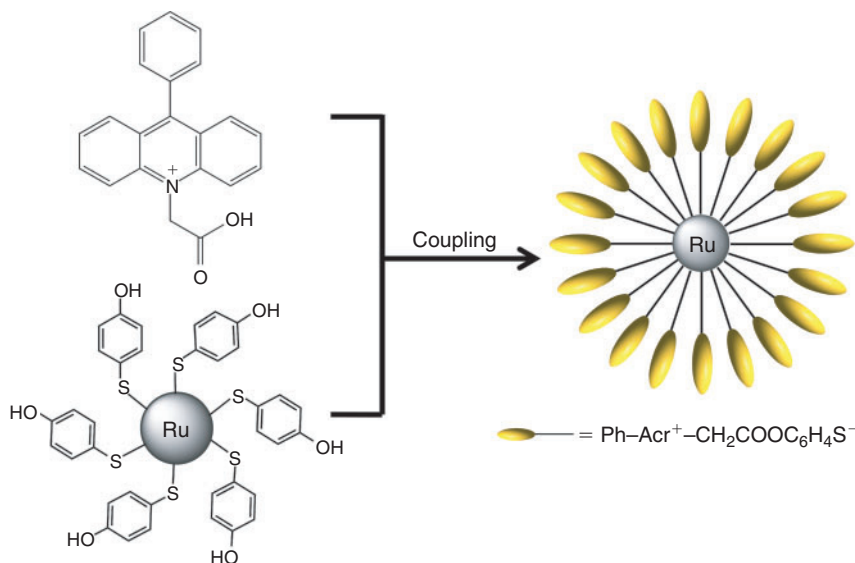


Fig. 3. Hydrogen-evolution rates normalized by the weights of hydrogen-evolution catalysts. The reaction was performed by photoirradiation ($\lambda > 420$ nm) of a mixed solution of an aqueous buffer (pH 4.5) and MeCN (1 : 1 (v/v)) containing $[\text{Ru}(\text{bpy})_3]^{2+}$ (0.20 mM), EDTA (1.0 mM) using $\text{Ph}-\text{Acr}^+-\text{Me}$ (0.30 mM) and RuNPs (0.10 g L^{-1}) or RuO_2NPs (0.25 g L^{-1}) or using PtNPs (0.025 g L^{-1}) and MV^{2+} (0.30 mM) as an electron mediator and a hydrogen-evolution catalyst.

as $92 \mu\text{mol s}^{-1} \text{g}_{\text{Pt}}^{-1}$, which is much larger than that of $4.2 \mu\text{mol s}^{-1} \text{g}_{\text{Ru}}^{-1}$ of the reaction system using RuNPs. However, when the hydrogen-evolution rates of the reaction systems using RuNPs ($4.2 \mu\text{mol s}^{-1} \text{g}_{\text{Ru}}^{-1}$) is compared with that of the reaction system using PtNPs and MV^{2+} ($7.1 \mu\text{mol s}^{-1} \text{g}_{\text{Pt}}^{-1}$), which is a typical photocatalytic hydrogen-evolution system, the hydrogen-evolution rate of the former is $\sim 60\%$ of the latter as shown in Fig. 3. The specific hydrogen-evolution rate of the reaction system using RuO_2NPs was $0.22 \mu\text{mol s}^{-1} \text{g}_{\text{RuO}_2}^{-1}$, which is very low, even compared with that of the conventional reaction system using PtNPs and MV^{2+} . These results suggest that RuNPs and RuO_2NPs act as hydrogen-evolution catalysts by using $\text{Ph}-\text{Acr}^+-\text{Me}$ as an electron mediator although further improvement is required in the catalytic reactivity.

Immobilization of an Electron Mediator on RuNPs

The immobilization of an electron mediator on the surfaces of RuNPs was examined by direct coupling of the carboxy-terminated 9-phenyl-10-methylcarboxyacridinium ion ($\text{Ph}-\text{Acr}^+-\text{CH}_2\text{COOH}$) with 4-mercaptophenol-functionalized RuNPs ($\text{HO}-\text{C}_6\text{H}_4\text{S}-\text{RuNPs}$), which is prepared by mixing 4-mercaptophenol and RuNPs in MeCN. $\text{Ph}-\text{Acr}^+-\text{CH}_2\text{COOH}$ acts as an electron mediator the same as $\text{Ph}-\text{Acr}^+-\text{Me}$ in the photocatalytic hydrogen-evolution system (Fig. A3 in the Supplementary Material). The coupling reaction was performed in the presence of N,N' -diisopropylcarbodiimide and 4-(N,N' -dimethylamino)-pyridinium-4-toluene-sulfonate as the coupling agents, as shown in Scheme 2.^[43] The immobilization of $\text{Ph}-\text{Acr}^+-\text{CH}_2\text{COOH}$ was qualitatively confirmed by the UV-vis measurement of the particles after the coupling reactions. Fig. 4a shows the characteristic bands of $\text{Ph}-\text{Acr}^+-\text{CH}_2\text{COOH}$ around 346, 362, and 430 nm and the characteristic band of $\text{HO}-\text{C}_6\text{H}_4\text{S}$ around 290 nm. The amount of $\text{Ph}-\text{Acr}^+-\text{CH}_2\text{COOH}$ immobilized on the surfaces of the RuNPs was estimated by thermal gravimetric (TG) measurements under atmospheric conditions (Fig. 4b). TG measurements for $\text{Ph}-\text{Acr}^+-\text{CH}_2\text{COOC}_6\text{H}_4\text{S}-\text{RuNPs}$ and $\text{HO}-\text{C}_6\text{H}_4\text{S}-\text{RuNPs}$ were performed by increasing the temperature from room temperature to 600°C with a ramp rate of $10^\circ\text{C min}^{-1}$. In the TG measurement for $\text{Ph}-\text{Acr}^+-\text{CH}_2\text{COOC}_6\text{H}_4\text{S}-\text{RuNPs}$, a sudden



Scheme 2. Preparation scheme for the $\text{Ph}-\text{Acr}^+-\text{CH}_2\text{COOC}_6\text{H}_4\text{S}-\text{RuNPs}$.

weight loss of 49 % was observed around 290°C, and successive weight loss was observed up to 500°C with a decrease of 16 % of total weight. Thus, the total weight loss observed for Ph-Acr⁺-CH₂COOC₆H₄S-RuNPs was 65 %. In the TG measurement for HO-C₆H₄S-RuNPs, the smaller weight loss of 57 % was observed by heating to 600°C with a steep weight loss of ~40 % around 250°C. Based on these weight-loss values, at least 17 % of the HOC₆H₄S⁻ moieties were reacted with Ph-Acr⁺-CH₂COOH (see the Supplementary Material for calculation procedures).

Fig. 5 compares the hydrogen-evolution rates normalized by catalyst weight determined for reaction systems using Ph-Acr⁺-CH₂COO-C₆H₄S-RuNPs (0.10 g_{Ru} L⁻¹ and ~0.18 mM for Ph-Acr⁺ moiety) with that using Ph-Acr⁺-CH₂COOH (0.30 mM) and HO-C₆H₄S-RuNPs (0.10 g_{Ru} L⁻¹). In both cases, the hydrogen evolution rates were significantly lower compared with that of the reaction system using RuNPs (0.10 g L⁻¹) and Ph-Acr⁺-Mes (0.30 mM). In particular, only a small amount of hydrogen was evolved from the solution using Ph-Acr⁺-CH₂COO-C₆H₄S-RuNPs. Thus, the coverage of RuNP surfaces by sulfur and the immobilization of the Ph-Acr⁺ moiety by -COO-C₆H₄S⁻ decelerates the hydrogen evolution. When Ph-Acr⁺-CH₂COOH was added to the reaction system using Ph-Acr⁺-CH₂COO-C₆H₄S-RuNPs, the hydrogen-evolution rate increased to the same level of that of the reaction system using RuNPs and Ph-Acr⁺-Mes. This result indicates that the linker of -CH₂COO-C₆H₄S⁻ is not suitable for immobilization of the Ph-Acr⁺ moiety. In a previous report, the 1-(1-hexyl-6-thiol)-1'-methyl-4,4'-bipyridinium ion (MVA²⁺) immobilized on Pt clusters acts as an efficient electron mediator for photocatalytic hydrogen evolution.^[44] From the comparison of the chemical structure of the electron mediators for immobilization (shown in Fig. A4 in the Supplementary Material), the distance between the acridinium and thiolate moieties of Ph-Acr⁺-CH₂COO-C₆H₄S⁻ is comparable to that between the pyridinium ion and thiolate of MVA²⁺. Thus, the rigid structure of the linker part (-CH₂COO-C₆H₄S⁻) may disturb efficient electron transfer from the acridinyl radical to RuNPs. These results suggest that improvement of metallic RuNPs by surface modification with organic molecules is not straightforward because of the less interactive nature of the metal surfaces with organic molecules.

Loading of Pt on RuO₂NPs and Immobilization of an Electron Mediator on Pt/RuO₂NPs

Pt particles supported on RuO₂NPs (Pt/RuO₂NPs) were examined as a hydrogen-evolution catalyst with Ph-Acr⁺-CH₂COOH instead of Ph-Acr⁺-Me as an electron mediator, because the carboxy group can be expected to interact with the metal oxide surface. Before catalysis measurements, the interaction between Ph-Acr⁺-COOH and RuO₂NP surfaces was

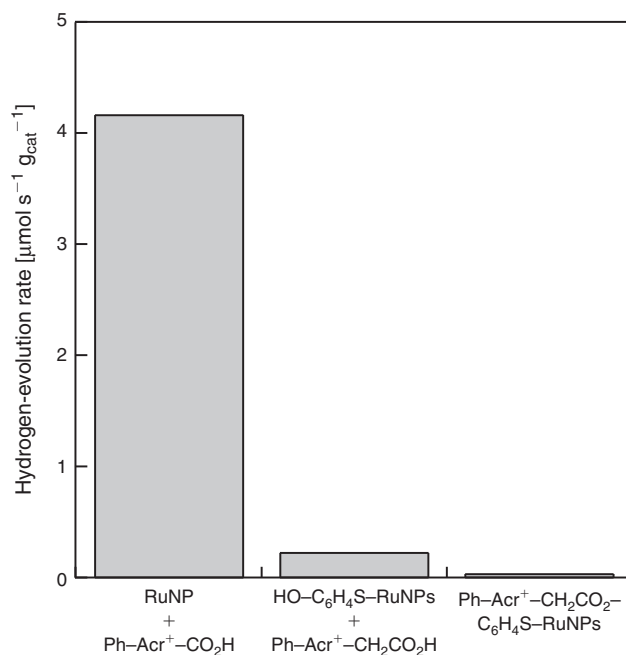


Fig. 5. Comparison of specific hydrogen-evolution rates normalized by the catalyst weight. Hydrogen evolutions were performed by photoirradiation ($\lambda > 420 \text{ nm}$) of the mixed solution (2.0 mL) of a phthalate buffer (pH 4.5) and MeCN (1:1 (v/v)) containing $[\text{Ru}(\text{bpy})_3]^{2+}$ (0.20 mM), EDTA (1.0 mM), and Ph-Acr-COOH (0.30 mM) and RuNPs (0.10 g_{Ru} L⁻¹), HO-C₆H₄S-RuNPs (0.10 g_{Ru} L⁻¹) and Ph-Acr-COOH (0.30 mM), or Ph-Acr⁺-CH₂COO-C₆H₄S-RuNPs (0.10 g_{Ru} L⁻¹, 0.17 mM of Ph-Acr⁺ moiety).

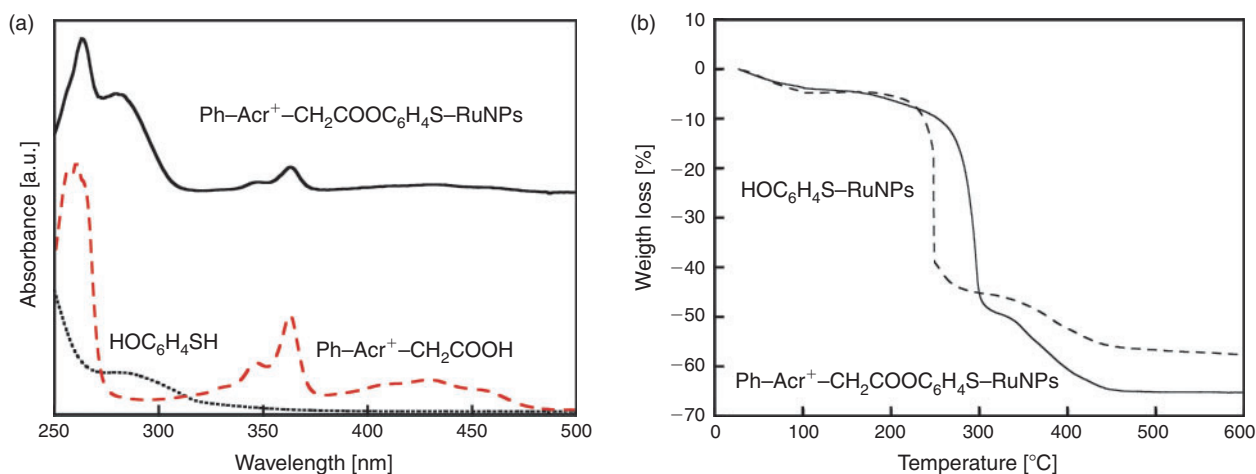


Fig. 4. (a) UV-vis spectra of Ph-Acr⁺-CH₂COOC₆H₄S-RuNPs (black solid), Ph-Acr⁺-CH₂COOH (red dashed), and HOC₆H₄SH (black dotted) in MeCN. (b) Thermal gravimetric curves of Ph-Acr⁺-CH₂COOC₆H₄S-RuNPs (black solid) and HOC₆H₄S-RuNPs (black dashed). The temperature was increased from room temperature to 600°C with a ramp rate of 10°C min⁻¹ under air.

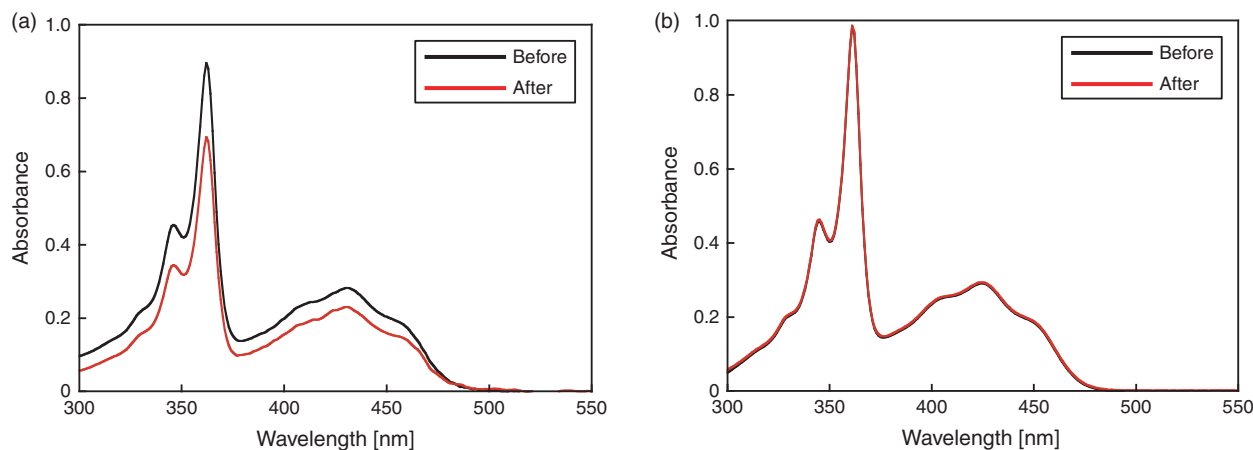


Fig. 6. (a) UV-vis spectra of Ph-Acr⁺-COOH in MeCN before and after addition of RuO₂NPs and (b) UV-vis spectra of Ph-Acr⁺-Me in MeCN before and after addition of RuO₂NPs.

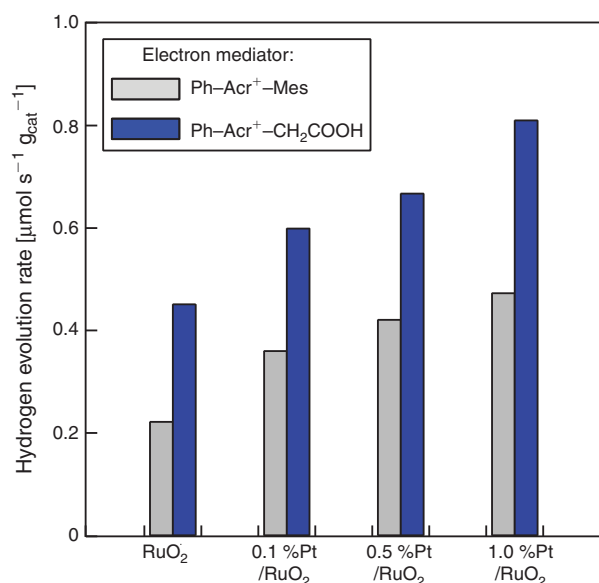


Fig. 7. Comparison of hydrogen-evolution rate normalized by catalyst weight in the photocatalytic hydrogen evolution using Pt/RuO₂ as hydrogen-evolution catalyst and Ph-Acr⁺-Mes (grey) or Ph-Acr⁺-CH₂COOH (blue) as an electron mediator. The loading amount of Pt on Pt/RuO₂ is 0.1, 0.5, or 1.0%. The hydrogen evolution was performed by photoirradiation ($\lambda > 420$ nm) of a mixed solution of a phthalate buffer (pH 4.5) and MeCN (1 : 1 (v/v)) containing [Ru(bpy)₃]²⁺ (0.20 mM), EDTA (1.0 mM), RuO₂NPs loaded with Pt (0.25 g_{RuO₂} L⁻¹), and Acr⁺-Ph-Me (0.30 mM) or Acr⁺-Ph-COOH (0.30 mM). Time courses of hydrogen evolution with each catalyst are indicated in Fig. A5 in the Supplementary Material.

directly confirmed by the UV-vis spectroscopic change as indicated in Fig. 6. RuO₂NPs (0.25 g L⁻¹) were added to a MeCN solution (2.0 mL) containing Ph-Acr⁺-COOH (0.05 mM) and slowly stirred for several minutes. The suspension was then slowly evaporated to dryness under reduced pressure and the same volume (2.0 mL) of MeCN was added to the residues. The UV-vis spectra were measured for the original solution and the supernatant solution after adsorption of Ph-Acr⁺-COOH on RuO₂NPs. As shown in Fig. 6a, the characteristic absorption bands of Ph-Acr⁺-CH₂COOH at 346, 362, and 430 nm decreased after the addition of RuO₂NPs. The decreases in absorption bands were ~20%. When the same

procedure was repeated with Ph-Acr⁺-Me instead of Ph-Acr⁺-CH₂COOH, no difference was observed in the UV-vis spectra before and after addition of RuO₂NPs. From the decrease in the absorbance, the amount of adsorbed Ph-Acr⁺-CH₂COOH was higher than 2.0×10^{-5} μmol , which corresponds to 280 molecules attached to one RuO₂NP under the assumption of a cylinder structure with a 10 nm diameter as the base and 20 nm in height.

Hydrogen evolution has been conducted using RuO₂NPs and Ph-Acr⁺-CH₂COOH as a hydrogen-evolution catalyst and an electron mediator by photoirradiation ($\lambda > 420$ nm). The hydrogen-evolution rate of $0.47 \mu\text{mol s}^{-1} \text{g}_{\text{RuO}_2}^{-1}$ determined for the reaction system was more than two times larger than that of $0.22 \mu\text{mol s}^{-1} \text{g}_{\text{RuO}_2}^{-1}$ determined for a reaction system using Ph-Acr⁺-Me as an electron mediator as shown in Fig. 7. The inefficient hydrogen evolution with RuO₂NPs even after the improvement indicates that RuO₂NPs are not suitable as a catalyst but a support material of Pt particles. A small amount of Pt metal was loaded on the surfaces of RuO₂NPs to evaluate RuO₂NPs as a support. The Pt metal was deposited on the surfaces of RuO₂NPs by reducing H₂PtCl₆ in ethanol, which is both solvent and reductant. Fig. 7 compares specific hydrogen-evolution rates normalized by weight of RuO₂NPs in the reaction systems using RuO₂ supporting different amounts of Pt as a hydrogen-evolution catalyst and Ph-Acr⁺-Me or Ph-Acr⁺-CH₂COOH as an electron mediator. The improvement in hydrogen-evolution rate by using Ph-Acr⁺-CH₂COOH was also observed in the reaction systems using Pt/RuO₂ as a hydrogen-evolution catalyst. When the loading amount of Pt was 0.10%, the hydrogen-evolution rates of 0.36 and $0.60 \mu\text{mol s}^{-1} \text{g}_{\text{cat}}^{-1}$ (normalized by total catalyst weight) were determined for the reaction systems using Ph-Acr⁺-Me and Ph-Acr⁺-CH₂COOH, respectively. When the hydrogen-evolution rates are normalized by the Pt weight of the catalysts, hydrogen-evolution rates are as high as 360 and $600 \mu\text{mol s}^{-1} \text{g}_{\text{Pt}}^{-1}$. As described above, the maximum hydrogen-evolution rate normalized by the Pt weight is $92 \mu\text{mol s}^{-1} \text{g}_{\text{Pt}}^{-1}$ when PtNPs were used as a hydrogen-evolution catalyst. The hydrogen-evolution rates of the reaction systems using Pt/RuO₂NPs increases in proportion to the loading amount of Pt. The hydrogen-evolution rates normalized by catalyst weight of the reaction systems using 0.5 and 1.0% Pt/RuO₂ with Ph-Acr⁺-CH₂COOH were 0.67 and $0.81 \mu\text{mol s}^{-1} \text{g}_{\text{cat}}^{-1}$ where the specific

hydrogen-evolution rates normalized by Pt weight were 133 and $81 \mu\text{mol s}^{-1} \text{g}_{\text{Pt}}^{-1}$. When Ph-Acr⁺-Me was employed as an electron mediator in these reaction systems, the hydrogen-evolution rates were decreased to 84 and $47 \mu\text{mol s}^{-1} \text{g}_{\text{Pt}}^{-1}$. Thus, improvement in the specific hydrogen rates by 50–80% was observed using Ph-Acr⁺-CH₂COOH instead of Ph-Acr⁺-Me as an electron mediator when RuO₂-based catalysts were used as hydrogen-evolution catalysts.

Conclusions

Highly efficient hydrogen evolution has been successfully achieved by photoirradiation ($\lambda > 420 \text{ nm}$) of a mixed solution of a phthalate buffer (pH 4.5) and MeCN (1 : 1 (v/v)) containing Ph-Acr⁺-Me as an electron mediator together with EDTA, [Ru(bpy)₃]²⁺, and PtNPs as a sacrificial electron donor, photosensitizer, and hydrogen-evolution catalyst, respectively. The hydrogen-evolution rate of this reaction system was more than 10 times higher than that of the reaction system using MV²⁺ as an electron mediator. The use of Ph-Acr⁺-Me as the electron mediator has enabled the use of Pt/RuO₂NPs and RuNPs as hydrogen-evolution catalysts instead of PtNPs. The electron mediator was immobilized on the surfaces of the hydrogen-evolution catalyst to examine the effect of immobilization on the electron-transfer rate from the electron mediator to the hydrogen-evolution catalyst. The introduction of a carboxylate group on the methyl group of Ph-Acr⁺-Me (Ph-Acr⁺-COO⁻) allowed interaction with the RuO₂NP surfaces. The hydrogen-evolution rate of the reaction system using Ph-Acr⁺-COO-RuO₂NPs was about two times larger than that of the system using Ph-Acr⁺-Me and RuO₂NPs. Such improvement in the hydrogen-evolution catalysis was also observed for Pt/RuO₂NPs in which the loading amount of Pt is lower than 0.5%. Ph-Acr⁺-COOH was successfully immobilized on the RuNPs surfaces by coupling with 4-mercaptophenol, which coordinate to RuNPs, however, no improvement in the hydrogen-evolution rate was observed. This result indicates that not only the distance between the redox centre of an electron mediator and the surface of RuNPs but also the rigidity of the linker is important.

Experimental

All chemicals used for synthesising ruthenium nanoparticles (RuNPs), ruthenium oxide nanoparticles (RuO₂NPs), and 9-phenyl-10-carboxymethylacridinium (Ph-Acr⁺-COOH) hexafluorophosphate were obtained from chemical companies and used without further purification. Ruthenium(III) chloride (RuCl₃·*n*H₂O, 38% Ru) and Pt-PVP nanoparticles (2 nm, PVP = poly(vinylpyrrolidone)) were supplied by Tanaka Kikinzoku Kogyo. Sodium borohydride, potassium hexafluorophosphate, hydrogen hexachloro platinate(IV) hexahydrate, pyridine, and dichloromethane were received from Wako Pure Chemicals. 9-Phenylacridine, *N*-methyl-9-acridone, EDTA disodium salt (EDTA), hydrogen bromide (30% in acetic acid, $\sim 5.1 \text{ mol L}^{-1}$), and trifluoromethanesulfonic anhydride were obtained from Tokyo Chemical Industry Co., Ltd. Benzyl glycolate was purchased from Sigma-Aldrich Co. Purified water was provided by a Millipore MilliQ water purification system where the electronic conductance was $18.2 \text{ M}\Omega \text{ cm}$. 9-Phenyl-10-carboxymethylacridinium hexafluorophosphate was synthesised by following the reported methods.^[41]

TEM images of nanoparticles, which were mounted on a copper microgrid coated with elastic carbon, were observed by a JEOL JEM 2100 operating at 200 keV. UV-vis spectra

were recorded by an Agilent UV8453 by using a quartz cuvette with 1.0 cm light-path length. TG/DTA analysis was performed with an SII nanotechnology EXSTAR 7000 under atmospheric conditions. Each sample was loaded in an Al pan (5 mm i.d.).

Synthesis of Nanoparticles (RuNPs, RuO₂NPs, and Pt/RuO₂)

Sodium borohydride (5.0 mmol, 0.20 g) was added to an aqueous solution (15 mL) containing ruthenium(III) chloride (0.20 mmol, 0.11 g) with vigorous stirring for 10 min. The obtained particles were collected by filtration and washed with pure water three times and dried under vacuum at room temperature. The metallic phase of RuNPs was confirmed by powder X-ray diffraction. The sizes of the obtained nanoparticles were determined by transmittance electron microscopy (TEM).

The RuO₂ nanoparticles (RuO₂NPs) were obtained by calcination of RuNPs under O₂ atmosphere at 600°C for 4 h. Formation of a RuO₂ phase was confirmed by powder X-ray diffraction. The sizes of the obtained nanoparticles were determined by TEM.

A calculated amount of hydrogen hexachloro platinate(IV) hexahydrate was dissolved in absolute ethanol (5 mL). RuO₂ was then immersed in the solution. The suspension was then refluxed for 3 h to reduce the platinum ions. The obtained powder was collected by filtration.

Synthesis of 9-Phenyl-10-carboxymethylacridinium Hexafluorophosphate (Ph-Acr⁺-CH₂COOH)(PF₆)

The triflate of benzyl glycolate was prepared by a reported method with slight modifications.^[43] Trifluoromethanesulfonic anhydride (1.84 mL, 11 mmol) was added to a CH₂Cl₂ solution (40 mL) of benzyl glycolate (1.66 g, 10 mmol) and pyridine (0.89 mL, 11 mmol) over a period of 5–10 min at –20°C. After complete addition, the reaction mixture was stirred for 30 min and warmed to room temperature and stirred for an additional 30 min. The reaction mixture was evaporated and rapidly passed through a short column of silica gel eluting with CH₂Cl₂. The fractions containing triflate were combined, the solvent was evaporated, and the residue was subjected to a second rapid chromatography (CH₂Cl₂/hexane, 1/1 (v/v)) to provide the triflate as a pale yellow oil which solidified at 0°C. This material was suitable for direct use without any further purification. The yellow solid (0.11 g, 0.37 mmol) was added to a CH₂Cl₂ solution (8.0 mL) of 9-phenylacridine (0.086 g, 0.34 mmol) over a period of 5–10 min at –15°C. After complete addition, the reaction mixture was stirred for 30 min, warmed to room temperature, and stirred for an additional 24 h. Dried diethyl ether was added to the reaction mixture and the precipitated crystals were filtered to yield 10-benzyloxycarbonylmethyl-9-phenylacridinium triflate. The acridinium ester protected by a benzyl group (0.15 g, 0.32 mmol) was suspended in a 30% solution of hydrogen bromide/acetic acid (3.5 mL, 18 mmol) and heated for 30 min at 50°C, and the solvent was removed under reduced pressure. The resulting solid was dissolved in 35 mL of distilled water and this was added to an aqueous solution (34 mL) of potassium hexafluorophosphate (3.0 g, 16 mmol). The resulting solution was stirred for 24 h at room temperature and precipitated crystals were filtered off to yield 9-phenyl-10-carboxymethylacridinium hexafluorophosphate.

Photocatalytic Hydrogen Evolution

Typical reaction procedures are as follows; RuO₂ catalyst (0.25 g L⁻¹) was added to a mixed solution (2.0 mL) of a phthalate buffer (50 mM, pH 4.5) and MeCN (1 : 1 (v/v)) containing EDTA (1 mM), [Ru(bpy)₃](ClO₄)₂ (0.2 mM), and Ph-Acr⁺-COOH (0.3 mM) in a reaction vial (3.0 mL) flushed with N₂ gas. The solution was then irradiated with a xenon lamp (Ushio Optical, Model X SX-UID 500X AMQ) through a colour filter glass (Asahi Techno Glass) transmitting λ > 420 nm at room temperature. Evolved hydrogen gas in the headspace was quantified by a Shimadzu GC-14B gas chromatograph (detector, TCD; column temperature, 50°C; column, active carbon with 60–80 mesh particles size; carrier gas, N₂).

Supplementary Material

UV-vis spectra of Ph-Acr⁺-Me and [Ru(bpy)₃]²⁺ (Fig. A1), time courses of hydrogen evolutions (Figs A2, A3 and A5), chemical structures of linkers (Fig. A4), and calculation procedure to estimate the ratio of reacted HO-C₆H₄-S⁻ are available as Supplementary Material on the Journal's website.

Acknowledgements

This work was supported by a Grant-in-Aid (Nos. 20108010 to SF and 24350069 to YY) from the Ministry of Education, Culture, Sports, Science and Technology, Japan, NRF/MEST of Korea through WCU (R312008-000-10010-0) and GRL (2010-00353) Programs (to SF). The authors acknowledge the Research Center for Ultra-Precision Science & Technology, Osaka University for TEM measurements and Prof. Norimitsu Tohnai for powder X-ray diffraction measurements.

References

- [1] S. Dunn, in *Encyclopedia of Energy* (Ed. C. J. Cleaveland) **2004**, Vol. 3, pp. 241–252 (Elsevier/Academic Press: San Diego, CA).
- [2] S. Fukuzumi, *Eur. J. Inorg. Chem.* **2008**, 1351. doi:10.1002/EJIC.200701369
- [3] M. Momirlan, T. N. Veziroglu, *Int. J. Hydrogen Energy* **2005**, *30*, 795. doi:10.1016/j.ijhydene.2004.10.011
- [4] S. Fukuzumi, Y. Yamada, T. Suenobu, K. Ohkubo, H. Kotani, *Energ. Environ. Sci.* **2011**, *4*, 2754.
- [5] G. Laurenczy, in *Encyclopedia of Catalysis* (Ed. I. T. Horvath) **2010** (Wiley-Interscience: Hoboken, NJ). doi:10.1002/0471227617.EOC111.PUB2
- [6] H. B. Gray, *Nat. Chem.* **2009**, *1*, 7. doi:10.1038/NCHEM.141
- [7] N. S. Lewis, D. G. Nocera, *Proc. Natl. Acad. Sci. USA* **2006**, *103*, 15729. doi:10.1073/PNAS.0603395103
- [8] D. G. Nocera, *Chem. Soc. Rev.* **2009**, *38*, 13. doi:10.1039/B820660K
- [9] (a) P. A. Brugger, P. Cuendet, M. Grätzel, *J. Am. Chem. Soc.* **1981**, *103*, 2923. doi:10.1021/JA00401A002
(b) C. K. Grätzel, M. Grätzel, *J. Am. Chem. Soc.* **1979**, *101*, 7741. doi:10.1021/JA00520A032
(c) K. Kalyanasundaram, J. Kiwi, M. Grätzel, *Helv. Chim. Acta* **1978**, *61*, 2720. doi:10.1002/HLCA.19780610740
(d) J. Kiwi, M. Grätzel, *Angew. Chem. Int. Ed.* **1979**, *18*, 624. doi:10.1002/ANIE.197906241
(e) J. Kiwi, M. Grätzel, *Nature* **1979**, *281*, 657. doi:10.1038/281657A0
(f) J. Kiwi, M. Grätzel, *J. Am. Chem. Soc.* **1979**, *101*, 7214. doi:10.1021/JA00518A015
(g) J. Kiwi, K. Kalyanasundaram, M. Grätzel, *Sol. Energ. Mater.* **1982**, *49*, 37. doi:10.1007/BFB0111292
- [10] H. B. Gray, A. W. Maverick, *Science* **1981**, *214*, 1201. doi:10.1126/SCIENCE.214.4526.1201
- [11] (a) G. M. Brown, B. S. Brunschwig, C. Creutz, J. F. Endicott, N. Sutin, *J. Am. Chem. Soc.* **1979**, *101*, 1298. doi:10.1021/JA00499A051
(b) S. F. Chan, M. Chou, C. Creutz, T. Matsubara, N. Sutin, *J. Am. Chem. Soc.* **1981**, *103*, 369. doi:10.1021/JA00392A022
(c) N. Sutin, C. Creutz, E. Fujita, *Comment. Inorg. Chem.* **1997**, *19*, 67. doi:10.1080/02603599708032729
- [12] (a) N. Toshima, *Pure Appl. Chem.* **2000**, *72*, 317. doi:10.1351/PAC200072010317
(b) N. Toshima, K. Hirakawa, *Polym. J.* **1999**, *31*, 1127. doi:10.1295/POLYMJ.31.1127
(c) N. Toshima, M. Kuriyama, Y. Yamada, H. Hirai, *Chem. Lett.* **1981**, *10*, 793. doi:10.1246/CL.1981.793
(d) N. Toshima, T. Yonezawa, *Makromol. Chem. Macromol. Symp.* **1992**, *59*, 281. doi:10.1002/MASY.19920590123
(e) N. Toshima, T. Yonezawa, *New J. Chem.* **1998**, *22*, 1179. doi:10.1039/A805753B
- [13] (a) T. Yonezawa, N. Toshima, *J. Mol. Catal.* **1993**, *83*, 167. doi:10.1016/0304-5102(93)87017-3
(b) I. Okura, N. Kimthuan, *J. Mol. Catal.* **1979**, *6*, 227. doi:10.1016/0304-5102(79)85004-X
(c) I. Okura, M. Takeuchi, N. Kimthuan, *Photochem. Photobiol.* **1981**, *33*, 413. doi:10.1111/J.1751-1097.1981.TB05439.X
(d) I. Okura, S. Aono, S. Kusunoki, *Inorg. Chim. Acta* **1983**, *71*, 77. doi:10.1016/S0020-1693(00)83641-5
- [14] (a) L. Persaud, A. J. Bard, A. Champion, M. A. Fox, T. E. Mallouk, S. E. Webber, J. M. White, *J. Am. Chem. Soc.* **1987**, *109*, 7309. doi:10.1021/JA00258A011
(b) D. L. Jiang, C. K. Choi, K. Honda, W. S. Li, T. Yuzawa, T. Aida, *J. Am. Chem. Soc.* **2004**, *126*, 12084. doi:10.1021/JA048912E
- [15] (a) Y. Amao, *ChemCatChem* **2011**, *3*, 458. doi:10.1002/CCTC.201000293
(b) N. Himeshima, Y. Amao, *Energy Fuels* **2003**, *17*, 1641. doi:10.1021/EF034006W
- [16] (a) S. Rau, B. Schafer, D. Gleich, E. Anders, M. Rudolph, M. Friedrich, H. Gorts, W. Henry, J. G. Vos, *Angew. Chem. Int. Ed.* **2006**, *45*, 6215. doi:10.1002/ANIE.200600543
(b) S. Tschierlei, M. Karnahl, M. Presselt, B. Dietzek, J. Guthmuller, L. Gonzalez, M. Schmitt, S. Rau, J. Popp, *Angew. Chem. Int. Ed.* **2010**, *49*, 3981. doi:10.1002/ANIE.200906595
(c) S. Tschierlei, M. Presselt, C. Kuhnt, A. Yartsev, T. Pascher, V. Sundstrom, M. Karnahl, M. Schwalbe, B. Schafer, S. Rau, M. Schmitt, B. Dietzek, J. Popp, *Chem.–Eur. J.* **2009**, *15*, 7678. doi:10.1002/CHEM.200900457
- [17] (a) H. Ozawa, M. A. Haga, K. Sakai, *J. Am. Chem. Soc.* **2006**, *128*, 4926. doi:10.1021/JA058087H
(b) H. Ozawa, M. Kobayashi, B. Balan, S. Masaoka, K. Sakai, *Chem. Asian J.* **2010**, *5*, 1860. doi:10.1002/ASIA.201000083
(c) H. Ozawa, K. Sakai, *Chem. Commun.* **2011**, *47*, 2227. doi:10.1039/C0CC04708B
(d) H. Ozawa, Y. Yokoyama, M. Haga, K. Sakai, *Dalton Trans.* **2007**, 1197. doi:10.1039/B617617H
(e) S. Tanaka, S. Masaoka, K. Yamauchi, M. Annaka, K. Sakai, *Dalton Trans.* **2010**, *39*, 11218. doi:10.1039/C0DT00741B
- [18] (a) M. Wang, Y. Na, M. Gorlov, L. Sun, *Dalton Trans.* **2009**, 6458. doi:10.1039/B903809D
(b) P. Zhang, M. Wang, J. Dong, X. Li, F. Wang, L. Wu, L. Sun, *J. Phys. Chem. C* **2010**, *114*, 15868. doi:10.1021/JP106512A
(c) P. Zhang, M. Wang, C. Li, X. Li, J. Dong, L. Sun, *Chem. Commun.* **2010**, *46*, 8806. doi:10.1039/C0CC03154B
(d) P. Zhang, M. Wang, Y. Na, X. Li, Y. Jiang, L. Sun, *Dalton Trans.* **2010**, *39*, 1204. doi:10.1039/B923159P
(e) W. Gao, J. Sun, M. Li, T. Åkermark, K. Romare, L. Sun, B. Åkermark, *Eur. J. Inorg. Chem.* **2011**, 1100. doi:10.1002/EJIC.201000872
- [19] M. Grätzel, *Acc. Chem. Res.* **1981**, *14*, 376. doi:10.1021/AR00072A003
- [20] (a) E. Amouyal, B. Zidler, P. Keller, A. Moradpour, *Chem. Phys. Lett.* **1980**, *74*, 314. doi:10.1016/0009-2614(80)85166-9
(b) E. Amouyal, B. Zidler, *Isr. J. Chem.* **1982**, *22*, 117.
- [21] P. Keller, A. Moradpour, E. Amouyal, B. Zidler, *J. Mol. Catal.* **1981**, *12*, 261. doi:10.1016/0304-5102(81)80013-2
- [22] C. Königstein, *J. Photochem. Photobiol. A* **1995**, *90*, 141. doi:10.1016/1010-6030(95)04091-S

- [23] C. V. Krishnan, N. Sutin, *J. Am. Chem. Soc.* **1981**, *103*, 2141. doi:10.1021/JA00398A066
- [24] C. V. Krishnan, B. S. Brunenschwig, C. Creutz, N. Sutin, *J. Am. Chem. Soc.* **1985**, *107*, 2005. doi:10.1021/JA00293A035
- [25] J. Hawecker, J.-M. Lehn, R. Ziessel, *Nouv. J. Chim.* **1983**, *7*, 271.
- [26] J.-M. Lehn, J. P. Sauvage, *Nouv. J. Chim.* **1977**, *1*, 449.
- [27] G. M. Brown, S. F. Chan, C. Creutz, H. A. Schwarz, N. Sutin, *J. Am. Chem. Soc.* **1979**, *101*, 7638. doi:10.1021/JA00519A040
- [28] S. F. Chan, M. Chou, C. Creutz, T. Matsubara, N. Sutin, *J. Am. Chem. Soc.* **1981**, *103*, 369. doi:10.1021/JA00392A022
- [29] M. Kirch, J.-M. Lehn, J. P. Sauvage, *Helv. Chim. Acta* **1979**, *62*, 1345. doi:10.1002/HLCA.19790620449
- [30] S. Harinipriya, M. V. Sangaranarayanan, *Langmuir* **2002**, *18*, 5572. doi:10.1021/LA025548T
- [31] (a) J. L. Dempsey, J. R. Winkler, H. B. Gray, *J. Am. Chem. Soc.* **2010**, *132*, 1060. doi:10.1021/JA9080259
(b) J. L. Dempsey, J. R. Winkler, H. B. Gray, *J. Am. Chem. Soc.* **2010**, *132*, 16774. doi:10.1021/JA109351H
(c) J. L. Dempsey, B. S. Brunenschwig, J. R. Winkler, H. B. Gray, *Acc. Chem. Res.* **2009**, *42*, 1995. doi:10.1021/AR900253E
- [32] (a) P. W. Du, K. Knowles, R. Eisenberg, *J. Am. Chem. Soc.* **2008**, *130*, 12576. doi:10.1021/JA804650G
(b) T. Lazarides, T. McCormick, P. W. Du, G. G. Luo, B. Lindley, R. Eisenberg, *J. Am. Chem. Soc.* **2009**, *131*, 9192. doi:10.1021/JA903044N
- [33] X. L. Hu, B. S. Brunenschwig, J. C. Peters, *J. Am. Chem. Soc.* **2007**, *129*, 8988. doi:10.1021/JA067876B
- [34] (a) B. Hinnemann, P. G. Moses, J. Bonde, K. P. Jorgensen, J. H. Nielsen, S. Horch, I. Chorkendorff, J. K. Nørskov, *J. Am. Chem. Soc.* **2005**, *127*, 5308. doi:10.1021/JA0504690
(b) H. I. Karunadasa, C. J. Chang, J. R. Long, *Nature* **2010**, *464*, 1329. doi:10.1038/NATURE08969
- [35] L. Loy, E. E. Wolf, *Sol. Energy* **1985**, *34*, 455. doi:10.1016/0038-092X(85)90019-2
- [36] (a) Y. Yamada, T. Miyahigashi, H. Kotani, K. Ohkubo, S. Fukuzumi, *J. Am. Chem. Soc.* **2011**, *133*, 16136. doi:10.1021/JA206079E
(b) Y. Yamada, T. Miyahigashi, H. Kotani, K. Ohkubo, S. Fukuzumi, *Energ. Environ. Sci.* **2012**, *5*, 6111.
- [37] H. Kotani, R. Hanazaki, K. Ohkubo, Y. Yamada, S. Fukuzumi, *Chem.–Eur. J.* **2011**, *17*, 2777. doi:10.1002/CHEM.201002399
- [38] E. Amouyal, P. Keller, A. Moradpour, *J. Chem. Soc., Chem. Commun.* **1980**, 1019. doi:10.1039/C39800001019
- [39] J. M. Kleijn, *Colloid Polym. Sci.* **1987**, *265*, 1105. doi:10.1007/BF01417469
- [40] E. Amouyal, *Sol. Energy Mater. Sol. Cells* **1995**, *38*, 249. doi:10.1016/0927-0248(95)00003-8
- [41] (a) K. Ohkubo, K. Suga, S. Fukuzumi, *Chem. Commun.* **2006**, 2018. doi:10.1039/B518127E
(b) K. Suga, K. Ohkubo, S. Fukuzumi, *J. Phys. Chem. A* **2005**, *109*, 10168. doi:10.1021/JP053465Q
- [42] (a) R. W. G. Wyckoff, *Crystal Structures* **1963**, 2nd edn (Interscience Publishers: New York, NY).
(b) W. H. Baur, A. A. Khan, *Acta Crystallogr. B* **1971**, *27*, 2133. doi:10.1107/S0567740871005466
- [43] S. Fukuzumi, R. Hanazaki, H. Kotani, K. Ohkubo, *J. Am. Chem. Soc.* **2010**, *132*, 11002. doi:10.1021/JA105314X
- [44] H. Kotani, K. Ohkubo, Y. Takai, S. Fukuzumi, *J. Phys. Chem. B* **2006**, *110*, 24047. doi:10.1021/JP065215V